

2D Materials



LETTER

Characterization of the second- and third-order nonlinear optical susceptibilities of monolayer MoS₂ using multiphoton microscopy

OPEN ACCESS

RECEIVED

15 August 2016

REVISED

12 October 2016

ACCEPTED FOR PUBLICATION

28 October 2016

PUBLISHED

29 November 2016

Original content from this work may be used under the terms of the [Creative Commons Attribution 3.0 licence](#).

Any further distribution of this work must maintain attribution to the author(s) and the title of the work, journal citation and DOI.



R I Woodward¹, R T Murray¹, C F Phelan², R E P de Oliveira², T H Runcorn¹, E J R Kelleher¹, S Li³, E C de Oliveira², G J M Fechine², G Eda³ and C J S de Matos²

¹ Femtosecond Optics Group, Department of Physics, Imperial College London, London, UK

² MackGraphe–Graphene and Nanomaterials Research Center, Mackenzie Presbyterian University, São Paulo, Brazil

³ Centre for Advanced 2D Materials, National University of Singapore, Singapore

E-mail: cjsdematos@mackenzie.br

Keywords: MoS₂, two-dimensional (2D) materials, second-harmonic generation, third-harmonic generation, multiphoton microscopy

Supplementary material for this article is available [online](#)

Abstract

We report second- and third-harmonic generation in monolayer MoS₂ as a tool for imaging and accurately characterizing the material's nonlinear optical properties under 1560 nm excitation. Using a surface nonlinear optics treatment, we derive expressions relating experimental measurements to second- and third-order nonlinear sheet susceptibility magnitudes, obtaining values of $|\chi_s^{(2)}| = 2.0 \times 10^{-20} \text{ m}^2 \text{ V}^{-1}$ and, for the first time for monolayer MoS₂, $|\chi_s^{(3)}| = 1.7 \times 10^{-28} \text{ m}^3 \text{ V}^{-2}$. These sheet susceptibilities correspond to effective bulk nonlinear susceptibility values of $|\chi_b^{(2)}| = 2.9 \times 10^{-11} \text{ m V}^{-1}$ and $|\chi_b^{(3)}| = 2.4 \times 10^{-19} \text{ m}^2 \text{ V}^{-2}$, accounting for the sheet thickness. Experimental comparisons between MoS₂ and graphene are also performed, demonstrating ~ 3.4 times stronger third-order sheet nonlinearity in monolayer MoS₂, highlighting the material's potential for nonlinear photonics in the telecommunications C band.

1. Introduction

Two-dimensional (2D) materials are attracting significant interest due to their unprecedented optical and electronic properties. While graphene remains the most widely studied 2D material, many other monolayer and few-layer atomic crystals possessing distinct yet complementary properties have recently been discovered [1, 2]. In particular, semiconducting few-layer transition metal dichalcogenides (TMDs), such as molybdenum disulfide (MoS₂), have received much attention. Few-layer MoS₂ exhibits ultrafast carrier dynamics, strong photoluminescence, saturable absorption and a bandgap which can be tuned by varying the number of atomic layers (from a 1.3 eV indirect gap for bulk MoS₂ to a direct 1.9 eV gap for a monolayer) [3–6]. These outstanding characteristics suggest the material has great potential as a platform for developing next-generation electronic, optoelectronic and photonic technologies, including transistors with current on/off ratios exceeding 10⁸,

ultrashort pulse lasers, flexible sensors and valleytronic devices [7–10].

As the catalogue of 2D materials continues to grow, an increasing need exists for a thorough and comparative characterization of their properties and performance. Nonlinear microscopy—a general term used to describe any microscopy technique that exploits a nonlinear optical interaction, including harmonic generation, four-wave mixing, and multiphoton absorption—has been demonstrated as a powerful tool for imaging and characterization of 2D atomic crystals [11–22]. Second harmonic generation (SHG) has been observed in monolayer and few-layer MoS₂ [16–20], and has been used to probe the crystal symmetry [18] and grain orientations [19] of fabricated samples. This technique, however, is limited to samples with an odd number of layers, as both bulk and even-layer-count few-layer crystals exhibit inversion symmetry; thus, second-order nonlinear effects are electric dipole forbidden. An attractive alternative is to harness third-harmonic generation (THG), which

occurs irrespective of inversion symmetry [12, 23, 24]. Wang *et al* recently reported THG from MoS₂ thin films of 7–15 atomic layers [21], suggesting THG could provide complementary information in multiphoton microscopy. Such a high layer count is approaching the bulk regime [1], however, and the technique has yet to be extended to single-layer MoS₂.

In addition to being a tool for crystal characterization, SHG and THG imaging are important techniques for evaluating fundamental material parameters, such as the nonlinear optical susceptibility tensors $\chi^{(2)}$ and $\chi^{(3)}$ that determine the strength of nonlinear processes, including the Pockels and Kerr effects, polarization rotation, frequency conversion, and phase conjugation—all of which define the usefulness of a material as a platform for the development of optical devices. Thus, it is crucial to characterize the nonlinearity of 2D materials, in particular at technologically relevant wavelengths, such as the telecommunications C band (1530–1565 nm), where emerging semiconductor materials could have major impact for on-chip switching and signal processing.

To relate experimental measurements to the magnitude of nonlinear susceptibility tensors, the 2D nature of monolayer atomic crystals must be considered. A variety of different formalisms have been adopted in literature to date to account for infinitesimally thin materials, leading to a wide variation in reported material properties: published values for $|\chi^{(3)}|$ in graphene, for example, vary by six orders of magnitude [25]. Further work is therefore needed to determine appropriate figures of merit for describing the nonlinear optical response of emerging 2D materials and to compare their performance.

Here, we determine the magnitude of the second- and third-order nonlinearity susceptibilities in monolayer MoS₂ using a power-calibrated multiphoton microscope setup by treating the 2D material as a nonlinear polarization sheet, adopting and extending established work on surface nonlinear optics [26]. We also characterize monolayer graphene, enabling a direct experimental comparison that shows MoS₂ possesses a stronger third-order nonlinear response and hence, could be more promising for practical nonlinear photonic applications.

2. Methods

First, monolayer MoS₂ flakes are fabricated by chemical vapor deposition (CVD) on a silicon (Si) substrate with a ~300 nm silica (SiO₂) coating layer, as described in [27]. Atomic force microscopy (AFM) and Raman microscopy are used to identify and characterize single-layer flakes (figures 1(a) and (b)), showing the expected ~0.7 nm thickness for a monolayer on the substrate and separation of ~19.4 cm⁻¹ between the E_{2g}¹ and A_{1g} Raman modes [28].

A microscope setup is developed to enable linear optical imaging using a green LED source and CCD camera in addition to measurement of harmonics that are generated when the sample is excited at normal incidence by a 1560 nm mode-locked Er: fiber laser (figure 2). Pump pulses with 150 fs duration at 89 MHz repetition rate are focussed through a 20× objective lens (0.50 NA) to a 1/e² diameter of 3.6 μm (with Rayleigh range ~ 6.5 μm). Pump light is linearly polarized and a half-waveplate (HWP) is included to control the incident polarization. Reflected harmonics can be observed overlaid on the linear optical image to identify the position of the pump light on the sample (figure 1(c)) or measured on a spectrometer. The sample is mounted on a piezo-controlled triaxial translation stage, enabling automated raster scanning across the material to construct the nonlinear images.

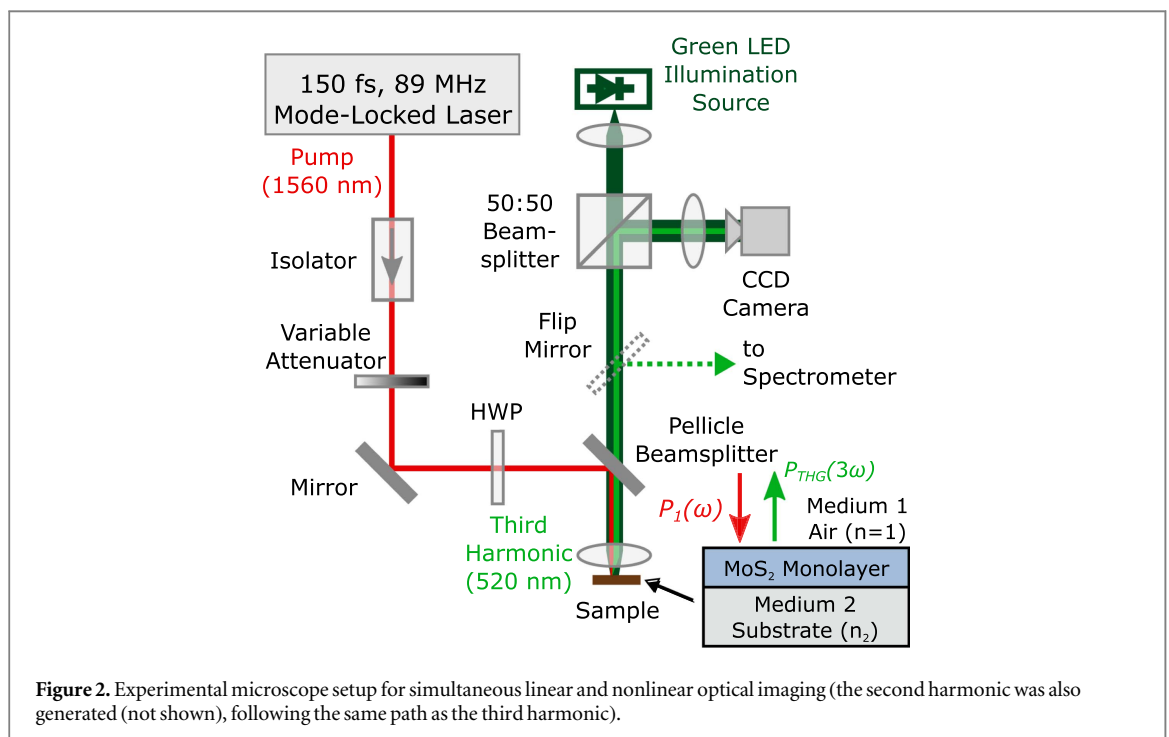
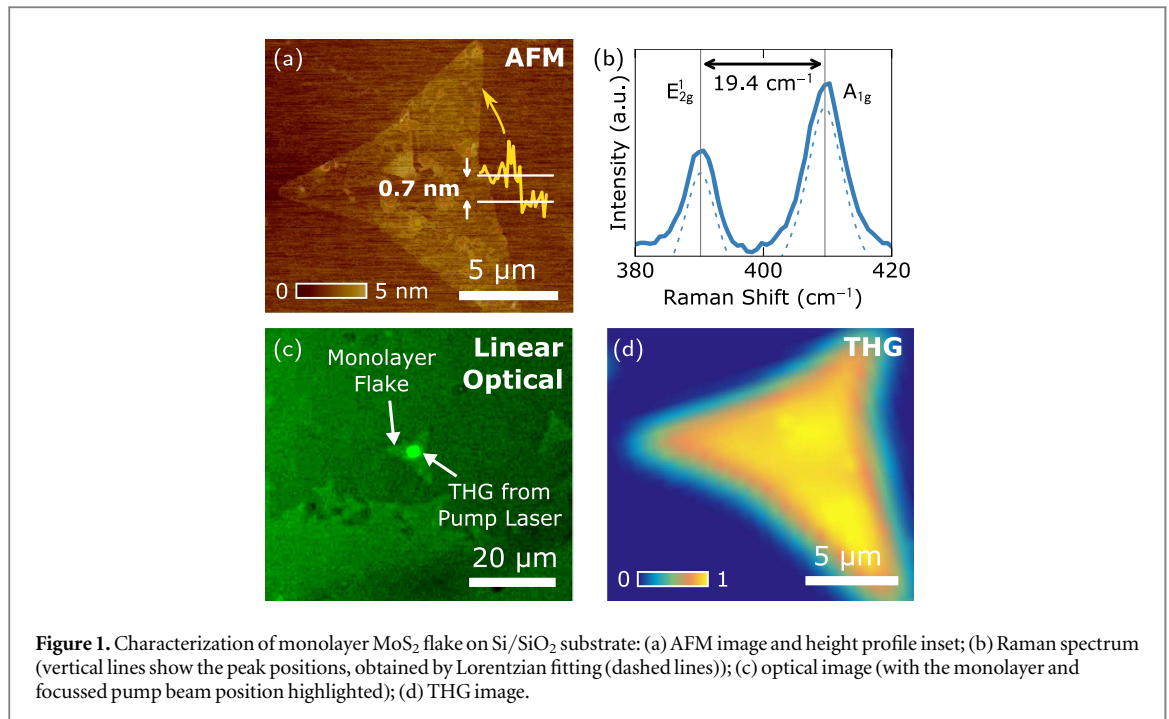
To relate measured intensity values using the spectrometer to the power at the sample, the system is carefully calibrated. The wavelength- and polarization-dependent transmission factors of all components are characterized using a white-light source, laser diode and polarizers, and accounted for in subsequent measurements. Finally, to verify the setup for quantifying nonlinear frequency conversion, the response of ZnS, a well-known bulk material, is measured, from which we obtain second- and third-order susceptibility values in good agreement with literature (see online supplementary information).

3. Results

3.1. MoS₂ characterization

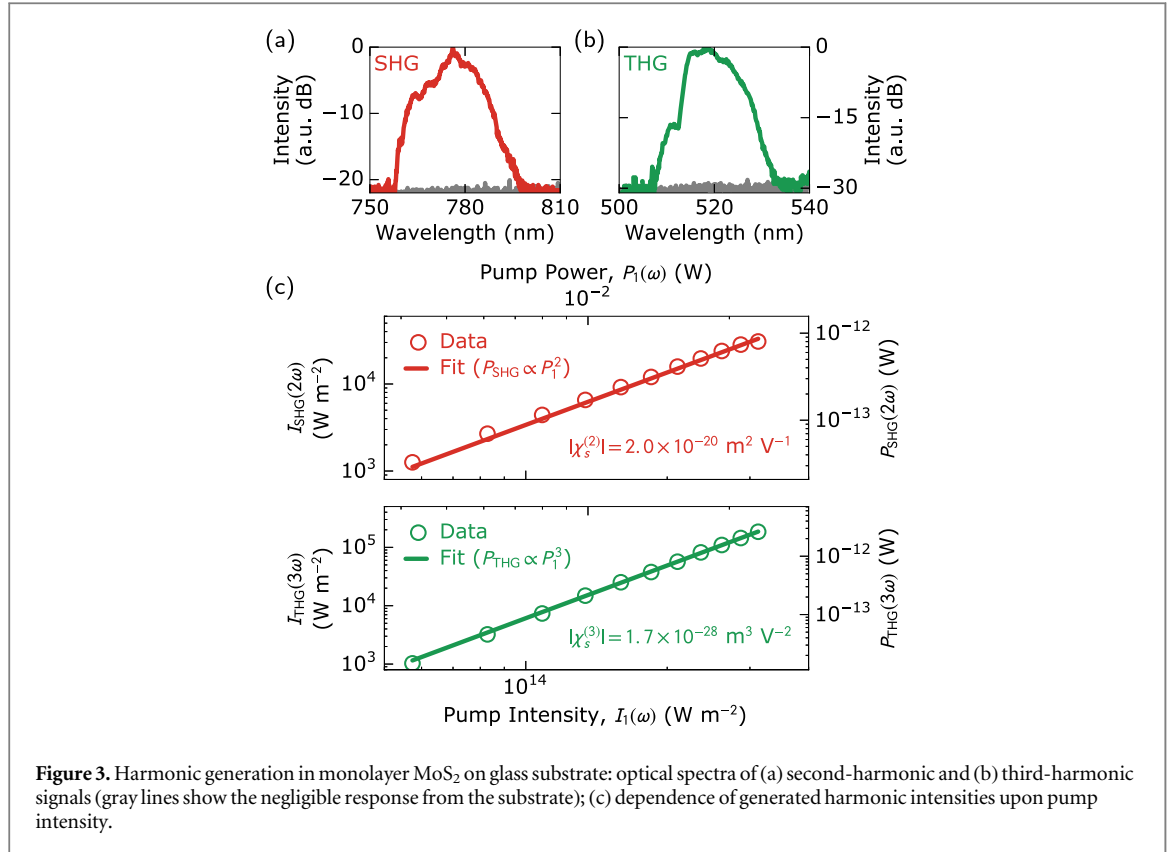
Second-harmonic (at 780 nm) and third-harmonic (at 520 nm) signals are clearly observed from monolayer MoS₂ flakes for an incident peak intensity of ~10¹⁴ W m⁻² (figures 3(a) and (b)). The sample geometry is imaged by raster scanning the pump beam position and recording the THG intensity (figure 1(d)), producing a higher contrast image than is possible with the linear optical microscopy part of the setup (figure 1(c)). We note that a similar image of monolayer MoS₂ could be obtained by recording the SHG intensity [16, 17], although the benefit of THG microscopy is that the technique is widely applicable to 2D materials with any number of layers, in addition to providing higher spatial resolution.

To quantify the nonlinear response of monolayer MoS₂, the modulus of the nonlinear susceptibility can be extracted from measurements of the intensity of generated harmonics compared to the pump. For this calculation we follow the theoretical surface SHG formalism of Shen [26]. Here, a surface is treated as a sheet of dipoles radiating coherently and nonlinearly, with a distinct dielectric constant and nonlinear susceptibility to the two materials meeting at the interface. Thus, the second-order nonlinear response of a



2D material is quantified by a nonlinear sheet susceptibility $|\chi_s^{(2)}|$ [17]. Local-field correction factors (i.e. Fresnel reflection coefficients) are also included to account for the boundary conditions. This approach is well suited to analysis of nonlinear optics in 2D materials where the infinitesimally small thickness not only indicates that no phase matching conditions apply along the direction normal to the sheet (and thus, to normally incident light), but also leads to nonlinearly radiated waves in both forwards and backwards directions. This latter feature cannot be obtained from a simple bulk nonlinear optics treatment.

In this work we apply this theory to monolayer MoS₂, treated as a nonlinear sheet at the interface between air and the dielectric substrate (figure 2), and expand the sheet polarization susceptibility formalism to THG in order to compute $|\chi_s^{(3)}|$. Our derivation (see online supplementary material) considers light at normal incidence to the sample and assumes negligible contribution from the nonlinearity of air or substrate, that the index of air is 1 and that the substrate dispersion is negligible (we also calculated susceptibility values including the effect of dispersion, obtaining <0.8% difference, verifying this assumption is a valid



simplification). SI units are used throughout. We find:

$$I_{\text{SHG}}(2\omega) = \frac{1}{\epsilon_0} \left[\frac{1}{2c} \left(\frac{2}{1+n_2} \right) \right]^2 (2\omega)^2 |\chi_s^{(2)}|^2 I_1^2(\omega) \quad (1)$$

and

$$I_{\text{THG}}(3\omega) = \frac{1}{\epsilon_0^2} \left[\frac{1}{2c} \left(\frac{2}{1+n_2} \right) \right]^4 (3\omega)^2 |\chi_s^{(3)}|^2 I_1^3(\omega), \quad (2)$$

where c is the speed of light in vacuum, ϵ_0 is the permittivity of free-space, $n_2 \sim 1.5$ is the substrate index, ω is the pump angular frequency, $I_1(\omega)$ is the focussed pump peak intensity in air, $|\chi_s^{(2)}|$ and $|\chi_s^{(3)}|$ are the magnitudes of the sheet susceptibility for second- and third-order nonlinearity, respectively. We relate peak intensities to experimentally measured time-averaged power values assuming Gaussian-shaped pulses and Gaussian beam optics, including correction factors to account for the pulse shortening and spot size reduction of the harmonics compared to the pump (see online supplementary material):

$$P_{\text{SHG}}(2\omega) = \frac{16\sqrt{2}S|\chi_s^{(2)}|^2\omega^2}{c^3\epsilon_0 f\pi r^2 t_{\text{fwhm}}(1+n_2)^6} P_1^2(\omega) \quad (3)$$

and

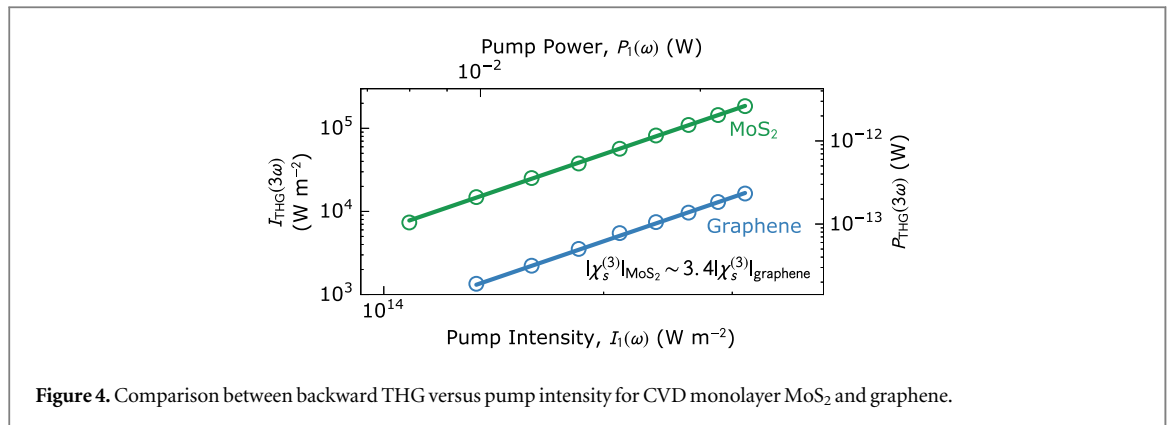
$$P_{\text{THG}}(3\omega) = \frac{64\sqrt{3}S^2|\chi_s^{(3)}|^2\omega^2}{c^4\epsilon_0^2(f t_{\text{fwhm}}\pi r^2)^2(1+n_2)^8} P_1^3(\omega), \quad (4)$$

where f is the pump laser repetition rate, $S = 0.94$ is a shape factor for Gaussian pulses, t_{fwhm} is the pulse full

width at half maximum, and $P_1(\omega)$ is the average pump power.

An Si substrate with ~ 300 nm SiO₂ overlayer is commonly chosen for 2D transition metal dichalcogenide crystal growth and inspection as it facilitates optical imaging for identifying few-layer samples, provided by an interferometrically enhanced contrast [2, 29]. However, interferometric effects from this layer could also enhance the measured backreflected harmonic generation [30], leading to an overestimate of the intrinsic nonlinearity of MoS₂ (as discussed and measured in the online supplementary material). Therefore, to avoid such effects, we transfer the MoS₂ monolayers to a transparent borosilicate glass substrate. The direct dry transfer method described in [31] is first used to transfer MoS₂ to poly(butylene-adipate-co-terephthalate) (PBAT), which is subsequently placed on the target substrate. The temperature is then raised until melting of the polymer and by using a solvent (chloroform), the polymer is completely removed.

The variation in generated harmonic power with variation in pump power for monolayer MoS₂ on the glass substrate shows that SHG and THG exhibit the expected quadratic and cubic dependences, respectively (figure 3(c)). From (3) and (4), we calculate $|\chi_s^{(2)}| = (2.0 \pm 0.4) \times 10^{-20} \text{ m}^2 \text{ V}^{-1}$ and $|\chi_s^{(3)}| = (1.7 \pm 0.6) \times 10^{-28} \text{ m}^3 \text{ V}^{-2}$ for monolayer MoS₂. The error values are obtained from measurement uncertainties of the terms in equations (3) and (4). Characterization experiments are repeated across 10 different monolayer flakes: we observe 3.7%



standard deviation relative to the mean value for the distribution of values of $|\chi_s^{(2)}|$ and 2.9% for $|\chi_s^{(3)}|$, suggesting good repeatability.

Finally, we note that monolayer MoS₂ belongs to the D_{3h} point group [18], which enables the polarization-dependence of harmonic generation to be determined from classical nonlinear optical theory [32]. This has already been verified for SHG [18]. We confirmed the expected polarization dependence of THG in a D_{3h} point group crystal for MoS₂ using a polarizer: for linearly polarized excitation, the emitted third-harmonic signal is collinearly polarized with the pump wave and as the pump polarization is varied from linear to circular using a quarter waveplate, the intensity of THG is reduced to zero (experimental results and theory are presented in supplementary material).

3.2. Comparison with graphene

As the array of available 2D materials grows, it is important to establish their relative nonlinear optical performance. Therefore, we compare the presented results with those for monolayer CVD graphene on a glass substrate, following an identical procedure used for MoS₂. This enables a direct comparison of harmonic generation between graphene and MoS₂ on the same substrate and in the same setup with 1560 nm excitation (figure 4). As expected from the inversion symmetry of graphene's atomic structure, SHG is not observed. We do observe THG in graphene, however, from which $|\chi_s^{(3)}| = (0.5 \pm 0.2) \times 10^{-28} \text{ m}^3 \text{ V}^{-2}$ is computed, suggesting that the third-order nonlinearity of MoS₂ is ~ 3.4 times greater.

This supports earlier observations of stronger saturable absorption, an additional nonlinear effect, in MoS₂ compared to graphene [5]. A further benefit of MoS₂ is the lack of inversion symmetry, enabling the exploitation of second-order effects (e.g. SHG [16–20] and sum-frequency generation [33]), which are absent in graphene. Monolayer MoS₂ could therefore be a superior material than graphene for nonlinear photonic applications at telecommunication wavelengths.

4. Discussion

A defining feature of monolayer TMDs is exciton effects, which can resonantly enhance light–matter interactions. In monolayer MoS₂, these excitonic transitions have previously been measured at 1.90 eV (653 nm), 2.05 eV (605 nm) and 2.8 eV (442 nm) [3, 17], labeled A, B and C according to standard nomenclature [34]. Previous SHG studies have reported an enhancement of nonlinear susceptibility values near these resonances: Malard *et al* measured an off-resonance second-order sheet susceptibility for mechanically exfoliated MoS₂ of $\sim 1 \times 10^{-20} \text{ m}^2 \text{ V}^{-1}$, increasing by a factor of ~ 8 as the SHG wavelength was shifted to overlap with the C exciton [17]. We note good agreement with our measured value of $|\chi_s^{(2)}| = 2 \times 10^{-20} \text{ m}^2 \text{ V}^{-1}$, for which no resonant enhancement is expected since both pump and second-harmonic are far from excitonic lines. Our 1560 nm pump wavelength is chosen for the potential to realize 2D material-based nonlinear optical devices for telecommunication applications. We note, however, that a stronger nonlinear response could be achieved at other salient pump wavelengths due to excitonic enhancement—e.g. for 1300 nm pumping, the second- and third-harmonic signals are expected to be resonant with the A and C excitons, respectively.

It should be noted that the fabrication method can affect the quality (i.e. defect content) of monolayer MoS₂. While mechanically exfoliated samples typically exhibit the highest quality, CVD is a more practical fabrication technique, which is scalable for high-yield production [35]. It is promising that our CVD MoS₂ monolayers exhibited similar nonlinear optical susceptibilities to the mechanically exfoliated MoS₂ of Malard *et al* [17]. We also verified this by producing monolayer MoS₂ using mechanical exfoliation [3] and comparing THG with that of a CVD sample under identical conditions: less than $\sim 26\%$ variation in the measured susceptibility value was noted. We conclude, therefore, that CVD MoS₂ can offer equivalent performance to mechanically exfoliated MoS₂ for nonlinear optical applications.

To compare to other literature reports, we relate our measured sheet susceptibilities to an effective bulk nonlinearity: $|\chi_b^{(n)}| = |\chi_s^{(n)}|/h$, where h is the monolayer thickness (0.7 nm for MoS₂, 0.335 nm for graphene [29]), yielding $|\chi_{b,MoS_2}^{(2)}| = 2.9 \times 10^{-11} \text{ m V}^{-1}$. This is within an order of magnitude of the $\sim 0.6 \times 10^{-11} \text{ m V}^{-1}$ value at 1560 nm excitation reported by Clark *et al*, who also tuned their pump wavelength to show a 7× and 5× enhancement in measured nonlinearity for MoS₂ on a silica substrate related to the A and B excitons, respectively [20]. Similar order-of-magnitude agreement is also noted with the off-resonance susceptibility value of $\sim 1 \times 10^{-10} \text{ m V}^{-1}$, derived by Trolle *et al* using tight-binding band structure theory including excitonic effects [36].

Our THG measurements are the first characterization of the third-order response of monolayer MoS₂ to the best of our knowledge. We note, however, that Wang *et al* have considered THG from multilayer (>7 layer) MoS₂ stacks, deducing an effective third-order susceptibility of $\sim 10^{-19} \text{ m}^2 \text{ V}^{-2}$ [21], which aligns with the bulk value of $|\chi_{b,MoS_2}^{(3)}| = 2.4 \times 10^{-19} \text{ m}^2 \text{ V}^{-2}$ that we derive from our sheet nonlinearity measurement. They suggest that enhancement due to band-to-band transitions occurs for all harmonic signals with photon energy exceeding the A exciton transition energy, with greatest enhancement near the A and B exciton. This is supported by their observation that THG is undetectable once the pump is tuned such that the third-harmonic wavelength exceeds $\sim 660 \text{ nm}$ [21].

It is also noteworthy that the generated third-harmonic intensity exceeds that of the second-harmonic. Conventionally, higher-order nonlinear processes are expected to be weaker as more photons are required for the interaction, which occurs with a lower probability. To explain our observation of a stronger THG signal, we note that the 520 nm emission may be enhanced by the edge of the B exciton, and it has also recently been suggested that for sufficiently low pump energies, the SHG signal strength may be decreased due to the energy bands taking part in the nonlinear process being nearly rotationally invariant, with only trigonal warping breaking inversion symmetry [37, 38].

Finally, we note that our graphene measurement results in an effective bulk value of $|\chi_{b,graphene}^{(3)}| = 1.5 \times 10^{-19} \text{ m}^2 \text{ V}^{-2}$. This was observed for graphene samples we fabricated using both CVD and mechanical exfoliation, and is notably four orders of magnitude weaker than reported by a four-wave mixing study by Hendry *et al* [11]. It has been noted, however, that a calculation error in [11] resulted in an overestimate [25]; when corrected, a value of $\sim 10^{-19} \text{ m}^2 \text{ V}^{-2}$ is obtained, in line with fundamental theoretical predictions [25] and also in agreement with our measured value.

5. Conclusion

We have comprehensively characterized the magnitude of both the second-order and, for the first time, third-order nonlinear susceptibility of monolayer MoS₂ using multiphoton microscopy. The 2D material was treated as a nonlinear polarization sheet, for which sheet susceptibility magnitudes of $|\chi_s^{(2)}| = 2.0 \times 10^{-20} \text{ m}^2 \text{ V}^{-1}$ and $|\chi_s^{(3)}| = 1.7 \times 10^{-28} \text{ m}^3 \text{ V}^{-2}$ were calculated from measurements, and direct experimental comparison between graphene and MoS₂ showed ~ 3.4 times stronger third-order nonlinearity in monolayer MoS₂. It was also shown that the nonlinear optical quality of CVD-grown MoS₂ was equivalent to mechanically exfoliated MoS₂. These results demonstrate opportunities for MoS₂ in integrated frequency conversion, nonlinear switching and signal processing, which depend on the magnitude of nonlinear susceptibilities we have characterized within the telecommunications C band.

Acknowledgments

We acknowledge funding from the São Paulo Research Foundation (FAPESP), grants 2012/50259-8, 2014/50460-0 and 2015/11779-4, and the Imperial College London Global Engagement Programme. This work is also partially funded by Conselho Nacional de Desenvolvimento Científico e Tecnológico (CNPq) and Fundo Mackenzie de Pesquisa (MackPesquisa). GE acknowledges Singapore National Research Foundation for funding under NRF Research Fellowship (NRF-NRFF2011-02) and Medium-Sized Centre Programme. CP, EJRK and RIW are supported by fellowships from FAPESP (grant 2015/12734-4), Royal Academy of Engineering and EPSRC, respectively.

References

- [1] Novoselov K S, Jiang D, Schedin F, Booth T J, Khotkevich V V, Morozov S V and Geim A K 2005 *Proc. Natl Acad. Sci. USA* **102** 10451–3
- [2] Wang Q H, Kalantar-Zadeh K, Kis A, Coleman J N and Strano M S 2012 *Nat. Nanotechnol.* **7** 699–712
- [3] Mak K F, Lee C, Hone J, Shan J and Heinz T F 2010 *Phys. Rev. Lett.* **105** 136805
- [4] Wang R, Ruzicka B A, Kumar N, Bellus M Z, Chiu H Y and Zhao H 2012 *Phys. Rev. B* **86** 045406
- [5] Wang K *et al* 2013 *ACS Nano* **7** 9260–7
- [6] Splendiani A, Sun L, Zhang Y, Li T, Kim J, Chim C Y, Galli G and Wang F 2010 *Nano Lett.* **10** 1271–5
- [7] Radisavljevic B, Radenovic A, Brivio J, Giacometti V and Kis A 2011 *Nat. Nanotechnol.* **6** 147–50
- [8] Woodward R I, Howe R C T, Hu G, Torrisi F, Zhang M, Hasan T and Kelleher E J R 2015 *Photon. Res.* **3** A30–42
- [9] Sarkar D, Xie X, Kang J, Zhang H, Liu W, Navarrete J, Moskovits M and Banerjee K 2015 *Nano Lett.* **15** 2852–62
- [10] Mak K F, He K, Shan J and Heinz T F 2012 *Nat. Nanotechnol.* **7** 494–8
- [11] Hendry E, Hale P J, Moger J, Savchenko A K and Mikhailov S A 2010 *Phys. Rev. Lett.* **105** 097401

- [12] Hong S Y, Dadap J I, Petrone N, Yeh P C, Hone J and Osgood R M 2013 *Phys. Rev. X* **3** 1–0
- [13] Janisch C, Wang Y, Ma D, Mehta N, Elías A L, Perea-López N, Terrones M, Crespi V and Liu Z 2014 *Sci. Rep.* **4** 5530
- [14] Susoma J, Karvonen L, Säynätjoki A, Mehravar S, Norwood R A, Peyghambarian N, Kieu K, Lipsanen H and Riikonen J 2016 *Appl. Phys. Lett.* **108** 073103
- [15] Karvonen L *et al* 2015 *Sci. Rep.* **5** 10334
- [16] Kumar N, Najmaei S, Cui Q, Ceballos F, Ajayan P, Lou J and Zhao H 2013 *Phys. Rev. B* **87** 161403
- [17] Malard L M, Alencar T V, Barboza A P M, Mak K F and de Paula A M 2013 *Phys. Rev. B* **87** 201401
- [18] Li Y, Rao Y, Mak K F, You Y, Wang S, Dean C R and Heinz T F 2013 *Nano Lett.* **13** 3329–33
- [19] Yin X, Ye Z, Chenet D A, Ye Y, O'Brien K, Hone J C and Zhang X 2014 *Science* **344** 488
- [20] Clark D J, Le C T, Senthilkumar V, Ullah F, Cho H Y, Sim Y, Seong M J, Chung K H, Kim Y S and Jang J I 2015 *Appl. Phys. Lett.* **107** 131113
- [21] Wang R, Chien H C, Kumar J, Kumar N, Chiu H Y and Zhao H 2014 *ACS Appl. Mater. Interfaces* **6** 314–8
- [22] Torres-Torres C, Perea-López N, Elías A L, Gutiérrez H R, Cullen D A, Berkdemir A, López-Urías F, Terrones H and Terrones M 2016 *2D Mater.* **3** 021005
- [23] Kumar N, Kumar J, Gerstenkorn C, Wang R, Chiu H Y, Smirl A L and Zhao H 2013 *Phys. Rev. B* **87** 121406
- [24] Woodward R I, Murray R T, Phelan C F, de Oliveira R E P, Li S, Eda G and de Matos C J S 2016 Characterization of the nonlinear susceptibility of monolayer MoS₂ using second- and third-harmonic generation microscopy *CLEO:2016* (OSA Technical Digest) p STu1R.3 (doi:10.1364/CLEO_SI.2016.STu1R.3)
- [25] Cheng J L, Vermeulen N and Sipe J E 2014 *New J. Phys.* **16** 053014
- [26] Shen Y 1989 *Annu. Rev. Phys. Chem.* **40** 327–50
- [27] van der Zande A M, Huang P Y, Chenet D A, Berkelbach T C, You Y, Lee G H, Heinz T F, Reichman D R, Muller D A and Hone J C 2013 *Nat. Mater.* **12** 554–61
- [28] Lee C, Yan H, Brus L E, Heinz T F, Hone J and Ryu S 2010 *ACS Nano* **4** 2695–700
- [29] Blake P, Hill E W, Castro Neto A H, Novoselov K S, Jiang D, Yang R, Booth T J and Geim A K 2007 *Appl. Phys. Lett.* **91** 198–201
- [30] Merano M 2015 *Opt. Lett.* **41** 187
- [31] Fehine G J M, Martin-Fernandez I, Yiapanis G, Bentini R, Kulkarni E S, de Oliveira R V B, Hu X, Yarovsky I, Neto A H C and Özyilmaz B 2014 *Carbon* **83** 224–31
- [32] Boyd R W 2007 *Nonlinear Optics* (New York: Academic)
- [33] Li D *et al* 2016 *ACS Nano* **10** 3766–75
- [34] Beal A R, Knights J C and Liang W Y 1972 *J. Phys. C: Solid State Phys.* **5** 3540
- [35] Schmidt H *et al* 2014 *Nano Lett.* **14** 1909–13
- [36] Trolle M L, Seifert G and Pedersen T G 2014 *Phys. Rev. B* **89** 235410
- [37] Kormanyos A, Zolyomi V, Drummond N D, Rakyta P, Burkard G and Fal'Ko V I 2013 *Phys. Rev. B* **88** 045416
- [38] Säynätjoki A *et al* 2016 arXiv:1608.04101